ACS Medicinal Chemistry Letters

Letter

pubs.acs.org/acsmedchemlett

^{18}F-Labeled Phenyldiazenyl Benzothiazole for in Vivo Imaging of Neurofibrillary Tangles in Alzheimer's Disease Brains

Kenji Matsumura,[†] Masahiro Ono,*[,†] Hiroyuki Kimura,[†] Masashi Ueda,[†] Yuji Nakamoto,[‡] Kaori Togashi,[‡] Yoko Okamoto,[§] Masafumi Ihara,[§] Ryosuke Takahashi,[§] and Hideo Saji[†]

[†]Department of Patho-Functional Bioanalysis, Graduate School of Pharmaceutical Sciences, Kyoto University, 46-29 Yoshida Shimoadachi-cho, Sakyo-ku, Kyoto 606-8501, Japan

[‡]Department of Diagnostic Imaging and Nuclear Medicine, Graduate School of Medicine, Kyoto University, 54 Shogoin-kawaharacho, Sakyo-ku, Kyoto 606-8507, Japan

[§]Department of Neurology, Graduate School of Medicine, Kyoto University, 54 Shogoin-kawaharacho, Sakyo-ku, Kyoto 606-8507, Japan

S *Supporting Information*

ABSTRACT: We synthesized and evaluated (*E*)-4-((6-(2-(2-(2-fluoroethoxy)ethoxy)ethoxy)benzo[*d*]thiazol-2-yl)-diazenyl)-*N*,*N*-dimethylaniline (FPPDB) as a probe for the imaging of neurofibrillary tangles (NFTs) in patients with Alzheimer's disease (AD). In assays using thioflavin S (ThS) as a competitive ligand, FPPDB competed with ThS well and showed high affinity for both tau and Aβ_{1-42} aggregates (K_i = 13.0 and 20.0 nM, respectively). The results of saturation binding assays also verified that FPPDB bound to both tau and Aβ_{1-42} aggregates with high affinity (K_d = 44.8 nM and B_{max} = 45.8 pmol/nmol protein for tau aggregates and K_d = 45.4 nM and B_{max} = 38.9 pmol/nmol protein for Aβ_{1-42} aggregates). Furthermore, [^{18}F]FPPDB substantially labeled NFTs and senile plaques in AD brain sections but not control brain sections. In biodistribution experiments using normal mice, [^{18}F]FPPDB displayed higher uptake (4.28% ID/g at 2 min postinjection) into and washout (2.53% ID/g at 60 min postinjection) from the brain with time. On the basis of the chemical structure of FPPDB, further increases in selective binding to tau aggregates may lead to the development of more useful probes for the imaging of NFTs in AD brains.

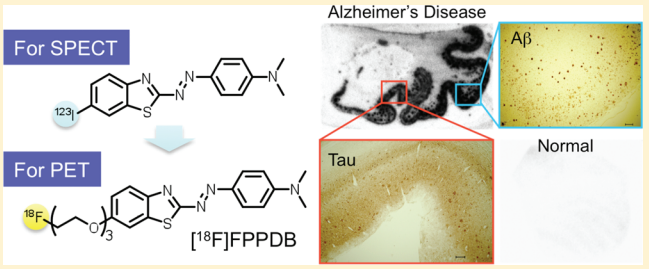

KEYWORDS: *Alzheimer's disease (AD), neurofibrillary tangles (NFTs), imaging, benzothiazole, PET*

Alzheimer's disease (AD) is a progressive neurodegenerative brain disorder associated with cognitive decline, disorientation, and language impairment and is characterized by the presence of senile plaques (SPs) composed of β-amyloid (Aβ) peptides and neurofibrillary tangles (NFTs) composed of hyperphosphorylated tau protein.[1] At present, the clinical diagnosis of AD depends on medical history and neuropsychological findings, and the early cognitive and behavioral symptoms of AD are often indistinguishable from normal signs of aging. Because a definite diagnosis of AD is based on the postmortem histopathological examination of SPs and NFTs, useful methods of evaluating the histopathological changes in vivo are strongly needed. The formation of SPs is considered an initial manifestation of AD. Therefore, considerable effort has focused on the development of imaging probes targeting SPs for positron emission tomography (PET) and single photon emission computed tomography (SPECT). Among them, PET/SPECT probes such as IMPY,[2] SB-13,[3] PIB,[4] AZD2184,[5] FDDNP,[6] BAY94-9172,[7] AV-45,[8] and GE-067[9] have been tested clinically and demonstrated the potential utility of the in vivo imaging of SPs in the brain. Many other compounds with structural similarities have also been reported.

Since the accumulation of NFTs is highly correlated with symptoms of AD[10,11] and the detection of NFTs in the brain should lead to the early diagnosis of AD and the evaluation of severity and staging, the development of NFT-selective binding probes is needed. However, there have been few reports on the development of PET/SPECT imaging probes targeting NFTs.

A previous paper has reported quinoline and benzimidazole derivatives as candidate probes for the imaging of NFTs in AD brains.[12,13] However, these derivatives showed affinity for both NFTs and SPs, suggesting that they may not be NFT-selective tracers. Therefore, to investigate the selective binding affinity for both NFTs and SPs, we recently developed radioiodinated compounds based on another chemical structure, a phenyldiazenyl benzothiazole (PDB) scaffold (Figure 1).[14] All of the PDB derivatives displayed high affinity for tau aggregates. PDB-

Received: September 23, 2011
Accepted: November 29, 2011
Published: December 1, 2011

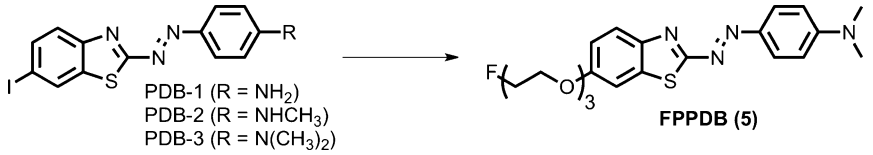

Figure 1. Chemical structure of iodinated and fluoro-pegylated PDB derivatives.

Scheme 1. [a]

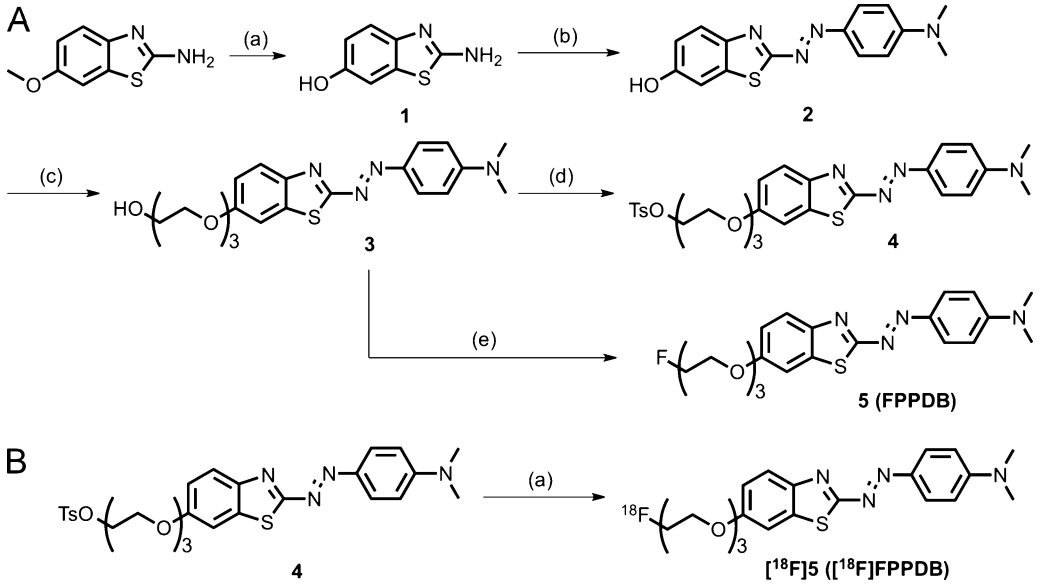

[a](A) Reagents and conditions: (a) HBr, reflux. (b) *N*,*N*-Dimethylaniline, $NaNO_2$, 50% H_2SO_4, concentrated HCl, 0 °C. (c) 2-[2-(2-Chloroethoxy)ethoxy]ethanol, K_2CO_3, DMF, 105 °C. (d) Tosyl chloride, pyridine. (e) Diethylamino sulfur trifluoride, 1,2-dimethoxyethane. (B) Reagents and conditions: (a) $^{18}F^-$, Kryptofix222, K_2CO_3, acetonitrile, 100 °C, 5 min.

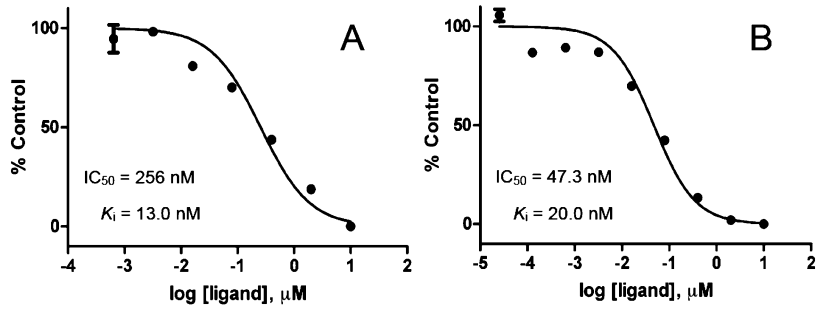

Figure 2. Inhibition curves for the binding of ThS to tau (A) and Aβ_{1-42} (B) aggregates using FPPDB as a test compound.

3, with a dimethylamino group at position 4 of the phenyl group, showed the highest affinity (17.2-fold that for Aβ_{1-42} aggregates), indicating it to be a tracer with greater selective binding to tau aggregates than the quinoline and benzimidazole derivatives reported previously. However, ^{125}I-labeled PDB derivatives showed a relatively low uptake into and slow washout from the brain, suggesting high nonspecific binding, which would contribute to a high level of background noise. Since the slow washout of [^{125}I]PDB derivatives in normal mice prevents imaging in vivo, the improved property of the PDB derivatives should make them better candidates for the study of tau aggregates.

Previous studies regarding uptake into and clearance from the brain points to high lipophilicity as one of the reasons for a slow washout.[15,16] We then planned to develop a novel PDB derivative with less lipophilicity by substituting iodine, which increases the lipophilicity of a compound, with fluorine for the preparation of PET tracers. Recent reports have introduced a new approach, fluoro-pegylation (FPEG) of the core structure, to labeling with ^{18}F.[7,17,18] Because this approach offers a simple and easy way to incorporate ^{18}F without any increase in lipophilicity, we selected FPEG for ^{18}F-labeling of the PDB scaffold. In the present study, we designed and synthesized a novel fluorinated ligand, (*E*)-4-((6-(2-(2-(2-fluoroethoxy)-ethoxy)ethoxy)benzo[*d*]thiazol-2-yl)diazenyl)-*N*,*N*-dimethylaniline (FPPDB, Figure 1) with a fluoro-polyethylene glycol side chain instead of iodine at position 6 of PDB-3, and evaluated its potential as a probe for the imaging NFTs in the brains in vivo.

A new ligand, FPPDB, was prepared as outlined in Scheme 1A. A methoxy group of 2-amino-6-methoxybenzothiazole was converted to a hydroxy group using a HBr solution, which afforded **1** in a yield of 71.0%. To obtain the backbone

dx.doi.org/10.1021/ml200230e | *ACS Med. Chem. Lett.* 2012, 3, 58–62

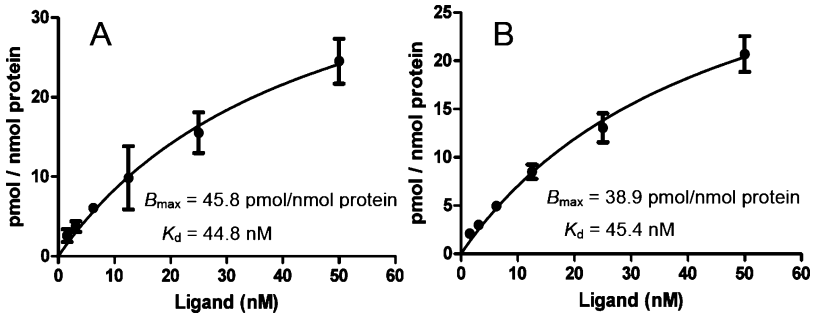

Figure 3. Saturation curves of [^{18}F]FPPDB for tau (A) and Aβ_{1-42} (B) aggregates.

structure of PDB, we used a diazo coupling reaction with *N*,*N*-dimethylaniline to afford **2**. Thereafter, 2-[2-(2-chloroethoxy)-ethoxy]ethanol was coupled with the OH group of **2** to obtain **3**. Fluorination of **3** to prepare **5** was achieved using diethylamino sulfur trifluoride (DAST). ^{18}F-labeling of **5** was performed on a tosyl precursor (**4**) undergoing a nucleophilic displacement reaction with the fluoride anion (Scheme 1B). Radiolabeling with ^{18}F was successfully performed on the precursor to generate [^{18}F]**5** ([^{18}F]FPPDB) with a radiochemical yield of 35% and radiochemical purity >99%. The identity of [^{18}F]FPPDB was verified by a comparison of retention time with the nonradioactive compound.

To evaluate the affinity of FPPDB for both tau aggregates and Aβ_{1-42} aggregates, an assay using thioflavin-S (ThS) as a competitive ligand was carried out. Similarly to iodinated PDB derivatives reported previously, FPPDB competed well with ThS to bind to tau aggregates (Figure 2A). The K_i value of FPPDB for tau aggregates was estimated at 13.0 nM. Although FPPDB exhibited significantly lower affinity than PDB-3 (K_i = 0.48 nM), it still maintained high enough affinity for tau aggregates to image NFTs. Because both tau and Aβ_{1-42} aggregates possess a β-sheet structure, it would be important to examine the selectivity of FPPDB. To this end, we determined the affinity of FPPDB for Aβ_{1-42} aggregates using a competitive inhibition assay with ThS. FPPDB also inhibited the binding of ThS to Aβ_{1-42} aggregates (Figure 2B), the K_i value being 20.0 nM. The ratio of the K_i values for tau and Aβ_{1-42} aggregates was 1.54. As compared to PDB-3 (ratio of 17.2),[14] FPPDB exhibited less selectivity between tau and Aβ_{1-42} aggregates. The results suggest that the substituted group at position 6 in the PDB scaffold plays an important role in the binding to β-sheet structures in both tau and Aβ_{1-42} aggregates. The concentration of tau aggregates (~150−300 pmol mg^{-1} of wet tissue) was reported to be higher than that of Aβ aggregates (~9 pmol mg^{-1} of wet tissue) in the frontal and temporal cortices in late-stage AD,[19,20] so it may be possible for [^{18}F]FPPDB to show contrast between NFTs and SPs in these areas in vivo. However, to diagnose AD in the early stages, probes with much higher NFT selectivity will be needed.

In competitive inhibition assays, FPPDB competed with ThS to bind to both tau and Aβ_{1-42} aggregates. To verify that FPPDB bound to these aggregates directly, saturation binding assays of [^{18}F]FPPDB to these aggregates were carried out (Figure 3). A Scatchard analysis revealed the K_d value and B_{max} of FPPDB for both tau and Aβ_{1-42} aggregates to be almost equal (K_d = 44.8 nM and B_{max} = 45.8 pmol/nmol tau protein for tau aggregates and K_d = 45.4 nM and B_{max} = 38.9 pmol/nmol Aβ_{1-42} protein for Aβ_{1-42} aggregates). This result showed that FPPDB had almost equal affinity for tau and Aβ_{1-42} aggregates, which was reflected the K_i values of FPPDB for both aggregates in the competitive inhibition assays using ThS.

[^{18}F]FPPDB was investigated for its affinity for NFTs in vitro by autoradiography in human AD brain sections (Figure 4).

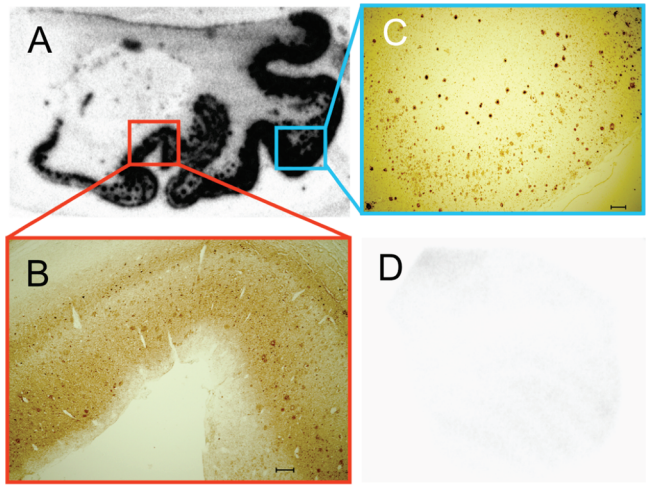

Figure 4. Autoradiogram of [^{18}F]FPPDB (A) and immunohistochemical staining with antibodies against hyperphosphorylated tau (B) and Aβ_{1-42} (C) in brain sections from the same patient. Autoradiogram of a control brain (D). Bars indicate 200 μm.

Autoradiographic images of [^{18}F]FPPDB showed the accumulation of radioactivity in the AD brain sections with little nonspecific binding in white matter (Figure 4A). The accumulation corresponded with the results of immunohistochemical staining with both the anti phosphorylated tau antibody (AT8) and the anti Aβ_{1-42} antibody (BC05) (Figure 4B,C, respectively). Conversely, [^{18}F]FPPDB showed almost no accumulation in normal human brain sections (Figure 4D). These results suggested that [^{18}F]FPPDB had enough affinity to label NFTs in AD brain sections, although its affinity for tau aggregates was lower than that of iodinated PDB derivatives. However, the results also indicated that [^{18}F]FPPDB did not possess enough selectivity for NFTs to show high contrast between NFTs and SPs in an autoradiographic study, similarly to the iodinated PDB derivatives reported previously.

To further confirm the affinity of FPPDB for NFTs and SPs in the AD brain, fluorescent staining was carried out using brain sections from the same AD patient (Figure 5). Numerous fluorescent spots were detected in the entorhinal cortex of AD brain sections (Figure 5A,C) as reflected by the high affinity for recombinant tau and Aβ_{1-42} aggregates in both competitive inhibition and saturation binding assays in vitro. ThS stained

dx.doi.org/10.1021/ml200230e | *ACS Med. Chem. Lett.* 2012, 3, 58−62

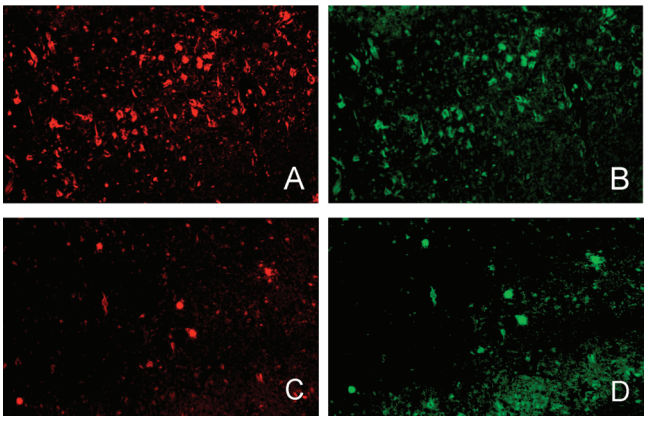

Figure 5. Fluorescent staining with FPPDB (A and C) and ThS (B and D) in the entorhinal cortex of AD brain sections. Many NFTs were clearly stained with FPPDB (A) and ThS (B). SPs were also stained with FPPDB (C) and ThS (D).

both NFTs (Figure 5B) and SPs (Figure 5D) clearly, and the fluorescent spots corresponded to those obtained with FPPDB (Figure 5A,C), suggesting that FPPDB bound to not only NFTs but also SPs.

To determine the uptake of [^{18}F]FPPDB in the brain, a biodistribution experiment was performed in normal mice (Table 1). [^{18}F]FPPDB displayed high uptake (4.28% ID/g) at 2 min postinjection, sufficient for PET imaging, and the radioactivity in the brain cleared with time. At 60 min postinjection, the uptake was 2.53% ID/g, indicating a relatively fast washout from the brain. Since normal brain tissue has neither NFTs nor SPs to trap [^{18}F]FPPDB, the radioactivity should wash out quite rapidly. Therefore, [^{18}F]FPPDB's rapid clearance from normal brain makes it more appropriate as an imaging agent for AD brain. [^{125}I]PDB-3 displayed less uptake into and a slower washout from the brain (0.94 and 2.89% ID/g at 2 and 60 min postinjection, respectively) than [^{18}F]-FPPDB.[14] The improved pharmacokinetics of [^{18}F]FPPDB were achieved by replacing iodine with a fluoro-pegylated group at position 6. The log *P* value of [^{18}F]FPPDB and [^{125}I]PDB-3 was 2.05 and 3.84, respectively, suggesting that [^{18}F]FPPDB is less lipophilic than [^{125}I]PDB-3. Although lipophilicity is just one of the factors influencing the uptake of a compound into the brain, it may explain in the favorable pharmacokinetics of [^{18}F]FPPDB. However, as compared with several Aβ imaging probes under clinical study such as [^{18}F]BAY94-9172[7] and [^{18}F]AV-45,[8] [^{18}F]FPPDB's uptake into and washout from the brain were not particularly satisfactory. The replacement of the dimethylamino group of [^{18}F]FPPDB with a less lipophilic group may lead to the development of more promising probes for diagnosing AD. Because defluorination, as reflected by the uptake of [^{18}F]FPPDB into bone, was low (1.82−1.92% ID/g), interference with the imaging is expected to be relatively minor. [^{18}F]FPPDB was cleared from plasma by not only the hepatobiliary system (20.2% ID/g in the liver at 2 min postinjection) but the renal system (13.9% ID/g in the kidney at 2 min postinjection). The hepatobiliary excretion to the intestines was also rather fast, and radioactivity was observed to accumulate within the intestine at later time points (22.9% ID/g at 60 min postinjection).

In conclusion, we designed, synthesized, and evaluated a PDB derivative, [^{18}F]FPPDB, as a novel PET imaging agent for diagnosing AD. In binding experiments in vitro, the derivative displayed high affinity for both tau and Aβ_{1-42} aggregates. NFTs and SPs were stained in experiments using autoradiography and fluorescent staining with AD brain sections, reflecting the results of the in vitro assays. Although FPPDB had lower selectivity for tau aggregates than PDB-3 in vitro, in biodistribution experiments using normal mice, [^{18}F]FPPDB had improved pharmacokinetics as compared with [^{125}I]PDB derivatives. Replacement of iodine with fluorine in the PDB scaffold was highly effective in improving the radioactive pharmacokinetics of [^{18}F]FPPDB in the brain. However, it resulted in a decrease in selective binding for tau aggregates. Further structural optimization based on the PDB scaffold, such as changing the position substituted in the fluoro-pegylated group or replacing the dimethylamino group with different groups to improve the affinity for tau aggregates may lead to the development of more useful probes for the in vivo imaging of NFTs in AD brains.

■ ASSOCIATED CONTENT

Supporting Information

Full experimental procedures and characterization data for all new compounds described in this study. This material is available free of charge via the Internet at http://pubs.acs.org.

Table 1. Biodistribution of Radioactivity after Injection of [^{18}F]FPPDB in Normal Mice[a]

	time after injection (min)			
tissue	2	10	30	60
blood	3.04 (0.40)	1.83 (0.82)	2.19 (0.75)	2.68 (0.63)
liver	20.2 (1.19)	19.3 (1.00)	13.1 (1.45)	9.32 (1.51)
kidney	13.9 (1.50)	7.67 (3.42)	5.08 (3.67)	4.00 (3.75)
intestine	2.94 (0.38)	4.99 (0.95)	14.4 (1.44)	22.9 (1.38)
spleen	3.47 (0.80)	3.41 (0.80)	2.71 (0.80)	2.14 (0.76)
pancreas	5.41 (0.69)	4.01 (1.03)	2.87 (0.63)	2.18 (0.67)
heart	7.45 (0.84)	4.14 (1.87)	3.05 (1.64)	2.62 (1.45)
lung	13.5 (3.51)	4.37 (4.60)	3.36 (3.70)	3.59 (3.18)
stomach[b]	1.11 (0.07)	1.42 (0.35)	2.69 (0.44)	3.37 (1.26)
brain	4.28 (0.45)	4.26 (0.37)	3.47 (0.54)	2.53 (0.54)
bone	1.88 (0.47)	1.82 (0.50)	1.82 (0.49)	1.92 (0.33)

[a]Each value represents the mean (SD) for five animals. [b]Expressed as % injected dose per organ.

dx.doi.org/10.1021/ml200230e | ACS Med. Chem. Lett. 2012, 3, 58−62

AUTHOR INFORMATION

Corresponding Author

*Tel: +81-75-753-4608. Fax: +81-75-753-4568. E-mail: ono@pharm.kyoto-u.ac.jp.

Funding

This study was supported by the Funding Program for Next Generation World-Leading Researchers (NEXT Program) and a Grant-in-aid for Young Scientists (A) and Exploratory Research from the Ministry of Education, Culture, Sports, Science and Technology, Japan.

Notes

The authors declare no competing financial interest.

ACKNOWLEDGMENTS

We thank Prof. Hiroshi Mori for kindly providing human tau cDNA for the in vitro binding assays.

REFERENCES

(1) Selkoe, D. J. Alzheimer's disease: Genes, proteins, and therapy. *Physiol. Rev.* **2001**, *81*, 741−766.

(2) Newberg, A. B.; Wintering, N. A.; Plossl, K.; Hochold, J.; Stabin, M. G.; Watson, M.; Skovronsky, D.; Clark, C. M.; Kung, M. P.; Kung, H. F. Safety, biodistribution, and dosimetry of ^{123}I-IMPY: a novel amyloid plaque-imaging agent for the diagnosis of Alzheimer's disease. *J. Nucl. Med.* **2006**, *47*, 748−754.

(3) Ono, M.; Wilson, A.; Nobrega, J.; Westaway, D.; Verhoeff, P.; Zhuang, Z. P.; Kung, M. P.; Kung, H. F. 11C-labeled stilbene derivatives as Aβ-aggregate-specific PET imaging agents for Alzheimer's disease. *Nucl. Med. Biol.* **2003**, *30*, 565−571.

(4) Klunk, W. E.; Engler, H.; Nordberg, A.; Wang, Y.; Blomqvist, G.; Holt, D. P.; Bergstrom, M.; Savitcheva, I.; Huang, G. F.; Estrada, S.; Ausen, B.; Debnath, M. L.; Barletta, J.; Price, J. C.; Sandell, J.; Lopresti, B. J.; Wall, A.; Koivisto, P.; Antoni, G.; Mathis, C. A.; Langstrom, B. Imaging brain amyloid in Alzheimer's disease with Pittsburgh Compound-B. *Ann. Neurol.* **2004**, *55*, 306−319.

(5) Johnson, A. E.; Jeppsson, F.; Sandell, J.; Wensbo, D.; Neelissen, J. A.; Jureus, A.; Strom, P.; Norman, H.; Farde, L.; Svensson, S. P. AZD2184: A radioligand for sensitive detection of β-amyloid deposits. *J. Neurochem.* **2009**, *108*, 1177−1186.

(6) Shoghi-Jadid, K.; Small, G. W.; Agdeppa, E. D.; Kepe, V.; Ercoli, L. M.; Siddarth, P.; Read, S.; Satyamurthy, N.; Petric, A.; Huang, S. C.; Barrio, J. R. Localization of neurofibrillary tangles and β-amyloid plaques in the brains of living patients with Alzheimer disease. *Am. J. Geriatr. Psychiatry* **2002**, *10*, 24−35.

(7) Zhang, W.; Oya, S.; Kung, M. P.; Hou, C.; Maier, D. L.; Kung, H. F. F-18 Polyethyleneglycol stilbenes as PET imaging agents targeting Aβ aggregates in the brain. *Nucl. Med. Biol.* **2005**, *32*, 799−809.

(8) Wong, D. F.; Rosenberg, P. B.; Zhou, Y.; Kumar, A.; Raymont, V.; Ravert, H. T.; Dannals, R. F.; Nandi, A.; Brasic, J. R.; Ye, W.; Hilton, J.; Lyketsos, C.; Kung, H. F.; Joshi, A. D.; Skovronsky, D. M.; Pontecorvo, M. J. In vivo imaging of amyloid deposition in Alzheimer disease using the radioligand ^{18}F-AV-45 (florbetapir F 18). *J. Nucl. Med.* **2010**, *51*, 913−920.

(9) Koole, M.; Lewis, D. M.; Buckley, C.; Nelissen, N.; Vandenbulcke, M.; Brooks, D. J.; Vandenberghe, R.; Van Laere, K. Whole-body biodistribution and radiation dosimetry of ^{18}F-GE067: A radioligand for in vivo brain amyloid imaging. *J. Nucl. Med.* **2009**, *50*, 818−822.

(10) Gomez-Isla, T.; Hollister, R.; West, H.; Mui, S.; Growdon, J. H.; Petersen, R. C.; Parisi, J. E.; Hyman, B. T. Neuronal loss correlates with but exceeds neurofibrillary tangles in Alzheimer's disease. *Ann. Neurol.* **1997**, *41*, 17−24.

(11) Arriagada, P. V.; Growdon, J. H.; Hedley-Whyte, E. T.; Hyman, B. T. Neurofibrillary tangles but not senile plaques parallel duration and severity of Alzheimer's disease. *Neurology* **1992**, *42*, 631−639.

(12) Okamura, N.; Suemoto, T.; Furumoto, S.; Suzuki, M.; Shimadzu, H.; Akatsu, H.; Yamamoto, T.; Fujiwara, H.; Nemoto, M.; Maruyama, M.; Arai, H.; Yanai, K.; Sawada, T.; Kudo, Y. Quinoline and benzimidazole derivatives: candidate probes for in vivo imaging of tau pathology in Alzheimer's disease. *J. Neurosci.* **2005**, *25*, 10857−10862.

(13) Fodero-Tavoletti, M. T.; Okamura, N.; Furumoto, S.; Mulligan, R. S.; Connor, A. R.; McLean, C. A.; Cao, D.; Rigopoulos, A.; Cartwright, G. A.; O'Keefe, G.; Gong, S.; Adlard, P. A.; Barnham, K. J.; Rowe, C. C.; Masters, C. L.; Kudo, Y.; Cappai, R.; Yanai, K.; Villemagne, V. L. ^{18}F-THK523: A novel in vivo tau imaging ligand for Alzheimer's disease. *Brain* **2011**, *134*, 1089−1100.

(14) Matsumura, K.; Ono, M.; Hayashi, S.; Kimura, H.; Okamoto, Y.; Ihara, M.; Takahashi, R.; Mori, H.; Saji, H. Phenyldiazenyl benzothiazole derivatives as probes for in vivo imaging of neurofibrillary tangles in Alzheimer's disease brains. *Med. Chem. Commun.* **2011**, *2*, 596−600.

(15) Cheng, Y.; Ono, M.; Kimura, H.; Kagawa, S.; Nishii, R.; Kawashima, H.; Saji, H. Fluorinated benzofuran derivatives for PET imaging of β-amyloid plaques in Alzheimer's disease brains. *ACS Med. Chem. Lett.* **2010**, *1*, 321−325.

(16) Ono, M.; Kawashima, H.; Nonaka, A.; Kawai, T.; Haratake, M.; Mori, H.; Kung, M. P.; Kung, H. F.; Saji, H.; Nakayama, M. Novel benzofuran derivatives for PET imaging of β-amyloid plaques in Alzheimer's disease brains. *J. Med. Chem.* **2006**, *49*, 2725−2730.

(17) Chandra, R.; Oya, S.; Kung, M. P.; Hou, C.; Jin, L. W.; Kung, H. F. New diphenylacetylenes as probes for positron emission tomographic imaging of amyloid plaques. *J. Med. Chem.* **2007**, *50*, 2415−2423.

(18) Stephenson, K. A.; Chandra, R.; Zhuang, Z. P.; Hou, C.; Oya, S.; Kung, M. P.; Kung, H. F. Fluoro-pegylated (FPEG) imaging agents targeting Aβ aggregates. *Bioconjug Chem* **2007**, *18*, 238−246.

(19) Wang, J.; Dickson, D. W.; Trojanowski, J. Q.; Lee, V. M. The levels of soluble versus insoluble brain Aβ distinguish Alzheimer's disease from normal and pathologic aging. *Exp. Neurol.* **1999**, *158*, 328−337.

(20) Khatoon, S.; Grundke-Iqbal, I.; Iqbal, K. Brain levels of microtubule-associated protein tau are elevated in Alzheimer's disease: A radioimmuno-slot-blot assay for nanograms of the protein. *J. Neurochem.* **1992**, *59*, 750−753.